On the formation of highly oxidized pollutants by autoxidation of terpenes under low temperature combustion conditions: the case of limonene and α-pinene.

Roland Benoit[1], Nesrine Belhadj[1,2], Zahraa Dbouk[1,2], Maxence Lailliau[1,2], and Philippe Dagaut[1]

[1]CNRS-INSIS, ICARE, Orléans, France, roland.benoit@cnrs-orleans.fr, nesrine.belhadj@cnrs-orleans.fr, zahraa.dbouk@cnrs-orleans.fr, maxence.lailliau@cnrs-orleans.fr, dagaut@cnrs-orleans.fr
[2]Université d'Orléans, Orléans, France

Correspondence: Roland Benoit (roland.benoit@cnrs-orleans.fr)

Author's track-changes : RC1, RC2, RC3

Abstract.

The oxidation of monoterpenes under atmospheric conditions has been the subject of numerous studies. They were motivated by the formation of oxidized organic molecules (OOM) which, due to their low vapor pressure, contribute to the formation of secondary organic aerosols (SOA). Among the different reaction mechanisms proposed for the formation of these oxidized chemical compounds, it appears that the autoxidation mechanism, involving successive events of O_2 addition and H-migration, common to both low-temperature combustion and atmospheric conditions, is leading to the formation of highly oxidized products (HOPs). However, cool flame oxidation (~500-800 K) of terpenes has not received much attention even if it can contribute to atmospheric pollution through biomass burning and wildfires. Under such conditions, terpenes can be oxidized via autoxidation. In the present work, we performed oxidation experiments with limonene-oxygen-nitrogen and α-pinene-oxygen-nitrogen mixtures in a jet-stirred reactor (JSR) at 590 K, a residence time of 2 s, and atmospheric pressure. Oxidation products were analyzed by liquid chromatography, flow injection, and soft ionization-high resolution mass spectrometry. H/D exchange and 2,4-dinitrophenyl hydrazine derivatization were used to assess the presence of OOH and C=O groups in oxidation products, respectively. We probed the effects of the type of ionization used in mass spectrometry analyses on the detection of oxidation products. Heated electrospray ionization (HESI) and atmospheric pressure chemical ionization (APCI), in positive and negative modes were used. We built an experimental database consisting of literature data for atmospheric oxidation and presently obtained combustion data for the oxidation of the two selected terpenes. This work showed a surprisingly similar set of oxidation products chemical formulas, including oligomers, formed under the two rather different conditions, i.e., cool flame and simulated atmospheric oxidation. Data analysis (in HESI mode) indicated that a subset of chemical formulas is common to all experiments, independently of experimental conditions. Finally, this study indicates that more than 45% of the detected chemical formulas in this full dataset can be ascribed to an autoxidation reaction.

1 Introduction

Terpenes are emitted into the troposphere by vegetation (Seinfeld and Pandis, 2006). They can be used as drop in fuels (Harvey et al., 2010;Mewalal et al., 2017;Harvey et al., 2015) which could increase emissions via fuel evaporation and unburnt fuel release. Biomass burning and wildfires can also release terpenes and their products of oxidation into the troposphere (Gilman et al., 2015;Hatch et al., 2019;Schneider et al., 2022). Wildfires temperature ranges from 573 to 1373 K (Wotton et al., 2012), which covers both the cool flame (~500-800 K) and intermediate to high temperature combustion regimes. Products of biomass burning have been characterized earlier (Smith et al., 2009). Using van Krevelen diagrams, the authors reported H/C versus O/C in the ranges 0.5 to 3 and 0 to 1, respectively. Whereas a large fraction of these products can derive from cellulose, hemicellulose, and lignin oxidation, their formation via terpenes oxidation cannot be ruled out. In a more recent study (Gilman et al., 2015), it was reported that biomass burning emissions were dominated by oxidized organic compounds (57 to 68% of total mass emissions). Wildfires are getting more and more frequent and their intensity increases(Burke et al., 2021). In large wildfires, there are many updrafts which can transport a variety of materials ranging from gases to particulates, and even bacteria (Kobziar et al., 2018). Furthermore, it was recently demonstrated that recent wildfires in Australia produced smoke which could reach an altitude of 35 km (Khaykin et al., 2020). Such events could contribute to ozone destruction (Bernath et al., 2022) but also to tropospheric pollution. But, field measurements are not appropriate for comparison with the present data because a strict distinction on the origins of the chemical compounds observed cannot be assessed. For example, literature works and reviews (Hu et al., 2018;Popovicheva et al., 2019;Prichard et al., 2020) present field measurements from smoldering fires which were not detailed enough to be used here.

Cool flame oxidation is dominated by autoxidation (Bailey and Norrish, 1952;Benson, 1981;Cox and Cole, 1985;Korcek et al., 1972) which involves peroxy radicals (ROO•). Autoxidation is based on an H-shift and oxygen addition which starts with the initial production of ROO• radicals. This mechanism can repeat itself several times and lead to recurrent oxygen additions to form highly oxidized products (Wang et al., 2017;Wang et al., 2018;Belhadj et al., 2020;Belhadj et al., 2021a;Belhadj et al., 2021b):

R•+ O_2 ⇄ ROO• (first O_2-addition)

ROO• ⇄•QOOH (H-shift)

•QOOH +O_2 ⇄ •OOQOOH (second O_2-addition)

•OOQOOH ⇄ HOOQ•'OOH (H-shift)

HOOQ•'OOH +O_2 ⇄ $(HOO)_2$Q'OO• (third O_2-addition)

$(HOO)_2$Q'OO• ⇄ $(HOO)_2$Q•"OOH (H-shift)

$(HOO)_2$Q•"OOH +O_2 ⇄ $(HOO)_3$Q"OO• (fourth O-addition), etc.

There, the formation of highly oxidized products (HOPs) was mainly attributed to autoxidation reactions (Belhadj et al., 2021c;Benoit et al., 2021).

In atmospheric chemistry, it is only relatively recently that this pathway has been considered (Vereecken et al., 2007;Crounse et al., 2013;Jokinen et al., 2014a;Ehn et al., 2014;Berndt et al., 2015;Jokinen et al., 2015;Berndt et al., 2016;Iyer et al., 2021). Also, it has been identified that highly oxygenated organic molecules (HOMs), a source of secondary organic aerosols (SOA), can result from autoxidation processes (Ehn et al., 2014;Wang et al.,

2021;Tomaz et al., 2021;Bianchi et al., 2019). Modeling studies complemented by laboratory experiments showed that autoxidation mechanisms proceed simultaneously on different ROO• radicals leading to the production of a wide range of oxidized compounds in a few hundredths of a second (Jokinen et al., 2014a;Berndt et al., 2016;Bianchi et al., 2019;Iyer et al., 2021). Recent works have shown that, under certain atmospheric conditions, this autoxidation mechanism could be competitive with other reaction pathways involving ROO• radicals (Bianchi et al., 2019), e.g., the carbonyl channel (ROO• → $R_{-H}O$ + OH), the hydroperoxide channel (ROO• + HOO• → ROOH + O_2 and RO• + •OH + O_2), disproportionation reactions (ROO• + R'OO• → RO• + R'O• + O_2 and $R_{-H}O$ + R'OH + O_2), accretion reactions (ROO• + R'OO• → ROOR' + O_2). Similarity, in terms of observed chemical formulas of products from cool flame oxidation of limonene and atmospheric oxidation of limonene, has been reported recently (Benoit et al., 2021). The same year, Wang et al. showed that the oxidation of alkanes follows this autoxidation mechanism under both atmospheric and combustion conditions (Wang et al., 2021). Also, that work confirmed that internal H-shifts in autoxidation can be promoted by the presence of functional groups, as predicted earlier (Otkjær et al., 2018) for ROO• radicals containing OOH, OH, OCH_3, CH_3, C=O, or C=C groups. Autoxidation will preferentially form chemical functions such as carbonyls, hydroperoxyl, or peroxyl. This large diversity of chemical functions will promote the formation of isomers. Nevertheless, the common point to these chemical compounds is the sequential addition of O_2. Therefore, in a database, potential candidate products of autoxidation are easily identified by this sequential addition.

To better understand the importance of these reaction pathways, the experimental conditions unique to these two chemistries must be considered. In laboratory studies conducted under simulated atmospheric conditions, oxidation occurs at near-ambient temperatures (250-300 K), at atmospheric pressure, in the presence of ozone and/or •OH radicals (Table S1), used to initiate oxidation with low initial terpene concentrations. In combustion, the •OH radical, temperature, and pressure are driving autoxidation. In addition to the increase in temperature, the initial concentrations of the reagents are generally higher compared to the atmospheric conditions, in order to initiate the oxidation with O_2, which is much slower than that involving ozone or •OH. Rising temperature increases isomerization rates and favors autoxidation, at the expense of other possible reactions of ROO• radicals. Indeed, it has been reported earlier that a temperature rise from 250 to 273K does not affect the distribution of HOMs (Quéléver et al., 2019) whereas Tröstl et al. suggested that the distribution of HOMs is affected by temperature, α-pinene or particle concentration (Tröstl et al., 2016). Similarly, the experiments of Huang et al. performed at different temperatures (223 K and 296 K) and precursor concentration (α-pinene 0.714 and 2.2 ppm) suggested that the physicochemical properties, such as the composition of the oligomers (at the nanometer scale), can be affected by a variation of temperature (Huang et al., 2018). The broad range of chemical molecules formed and the impact of the experimental conditions on their character remains a subject for atmospheric chemistry as well as for combustion chemistry studies. Whatever the mechanism of aerosols formation, i.e., oligomerization, functionalization, or accretion, their composition will be linked to that of the initial radical pool (Camredon et al., 2010;Meusinger et al., 2017;Tomaz et al., 2021).

In low-temperature combustion, when the temperature is increased, fuel's autoxidation rate goes through a maximum between 500 and 670 K, depending on the nature of the fuel (Belhadj et al., 2020;Belhadj et al., 2021c). In low-temperature combustion chemistry as in atmospheric chemistry, the oxidation of a chemical compound leads to the formation of several thousands of chemical products which result from successive additions of oxygen, isomerization, accretion, fragmentation, and oligomerization (Benoit et al., 2021;Belhadj et al., 2021b). The

exhaustive analysis of chemical species remains, under the current instrumental limitations, impossible. Indeed, this would consist in analyzing several thousands of molecules using separative techniques such as ultra-high-pressure liquid chromatography (UHPLC) or ion mobility spectrometry (IMS) (Krechmer et al., 2016;Kristensen et al., 2016). Nevertheless, it is possible to classify these molecular species, considering only $C_xH_yO_z$ compounds, according to criteria accessible via graphic tools representation such as van Krevelen diagrams, double bond equivalent number (DBE), and average carbon oxidation state (OSc) versus the number of carbon atoms (Kourtchev et al., 2015;Nozière et al., 2015). Such postprocessing of large datasets has the advantage of immediately highlighting classes of compounds or physicochemical properties such as the condensation of molecules (vapor pressure), the large variety of oxidized products ($C_xH_yO_{1\ to\ 15}$ in the present experiments) and the formation of oligomers (Kroll et al., 2011;Xie et al., 2020).

In addition to the recent studies focusing on the first steps of autoxidation, a more global approach, based on the comparison of possible chemical transformations related to autoxidation in low temperature combustion and atmospheric chemistry, is needed for evaluating the importance of autoxidation under tropospheric and low-temperature combustion conditions. In order to study the effects of experimental conditions on the diversity of chemical molecules formed by autoxidation, we have selected α-pinene and limonene, two isomeric terpenes among the most abundant in the troposphere (Zhang et al., 2018). Limonene has a single ring structure and two double bonds, one of which is exocyclic. α-Pinene has a bicyclic structure and a single endo-cyclic double bond. These two isomers with their distinctive physicochemical characters are good candidates for studying autoxidation versus initial chemical structure and temperature. For α-pinene, in addition to the reactivity of its endo-cyclic double bond, products of ring opening of the cyclobutyl group have been detected (Kurtén et al., 2015;Iyer et al., 2021), which could explain the diversity of observed oxidation products. This large pool of oxidation products is increased in the case of limonene by the presence of two double bonds (Hammes et al., 2019;Jokinen et al., 2015).

The present work extends that concerning the oxidation of limonene alone (Benoit et al., 2021). Compared to previous works, we have added the study of α-pinene oxidation to that of limonene and investigated the impact of ionization modes on the number of molecules detected and their chemical nature (unsaturation, oxidation rate). The size of the experimental and bibliographic databases has been increased by more than 50%, in particular by adding data specific to autoxidation (Krechmer et al., 2016;Tomaz et al., 2021) and references on α-pinene (Tab. 2)). Here, we oxidized α-pinene and limonene in a jet-stirred reactor at atmospheric pressure, excess of oxygen, and elevated temperature. We characterized the impact of using different ionization techniques (HESI and APCI) in positive and negative modes on the pool of detected chemical formulas. The particularities of each ionization mode were analyzed to identify the most suitable ionization technique for exploring the formation of autoxidation products under low temperature combustion. H/D exchange and 2,4-dinitrophenyl hydrazine derivatization were used to assess the presence of hydroperoxy and carbonyl groups, respectively. Chemical formulas detected here and in atmospheric chemistry studies were compiled and tentatively used to evaluate the importance of autoxidation routes under both conditions.

2 Experiments

2.1 Oxidation experiments

The present experiments were carried out in a fused silica jet-stirred reactor (JSR) setup presented earlier (Dagaut et al., 1986;Dagaut et al., 1988) and used in previous studies (Dagaut et al., 1987;Benoit et al., 2021;Belhadj et al., 2021c). We studied separately the oxidation of the two isomers, α-pinene and limonene. As in earlier works (Benoit et al., 2021;Belhadj et al., 2021c), α-pinene (+), 98% pure from Sigma Aldrich and limonene (R)-(+), >97% pure from Sigma Aldrich, were pumped by an HPLC pump (Shimadzu LC10 AD VP) with an online degasser (Shimadzu DGU-20 A3) and sent to a vaporizer assembly where it was diluted by a nitrogen flow. Each terpene isomer and oxygen, both diluted by N_2, were sent separately to a 42 mL JSR to avoid oxidation before reaching 4 injectors (nozzles of 1 mm I.D.) providing stirring. The flow rates of nitrogen and oxygen were controlled by mass flow meters. Good thermal homogeneity along the vertical axis of the JSR was recorded (gradients of < 1 K/cm) by thermocouple measurements (0.1 mm Pt-Pt/Rh-10% wires located inside a thin-wall silica tube). In order to observe the oxidation of these isomers, which are not prone to strong self-ignition, the oxidation of 1% of these chemical compounds ($C_{10}H_{16}$) under fuel-lean conditions (equivalence ratio 0.25, 56% O_2, 43% N_2), was carried out at 590 K, atmospheric pressure, and a residence time of 2 s. Under these conditions, the oxidation of the two isomers is initiated by slow H-atom abstraction by molecular oxygen ($RH + O_2 \rightarrow R^{\bullet} + HO_2^{\bullet}$). The fuel radicals $R^{\bullet}$ react rapidly with O_2 to form peroxy radicals which undergo further oxidation, characteristic of autoxidation. Nevertheless, this autoxidation mechanism, although predominant, is not exclusive and other oxidation mechanisms are possible (Belhadj et al., 2021b). In this case, there may be a random overlap of chemical formulas. The autoxidation criteria (two chemical formulas separated by two oxygen atoms) allows to limit or avoid these overlaps.

2.2 Chemical analyses

A 2 mm I.D. probe was used to collect samples. To measure low-temperature oxidation products ranging from early oxidation steps to highly oxidized products, the samples were bubbled into cooled acetonitrile (UHPLC grade ≥99.9, T= 0°C, 250 mL) for 90 min. The resulting solution was stored in a freezer at -15°C. The stability of the products was verified. No detectable changes in the mass spectra were observed after more than one month which is consistent with previous findings (Belhadj et al., 2021c).

Analyses of samples collected in acetonitrile (ACN) were carried out via direct infusion (rate: 3µL/min and recorded for 1 min for data averaging) in the ionization chamber of a high-resolution mass spectrometer (Thermo Scientific Orbitrap® Q-Exactive, mass resolution 140,000 and mass accuracy <0.5 ppm RMS). UHPLC conditions were: a Vanquish UHPLC Thermo Fisher Scientific with a C18 column (Phenomenex Luna, 1.6 µm, 110 Å, 100x2.1 mm). The column temperature was maintained at 40°C. 3µml of sample were eluted by mobile phase containing water-ACN mix (pure water, ACN HPLC grade) at a flow rate of 250 µL/min (gradient: 5% to 20% ACN -3 min, 20% to 65% ACN - 22 min, 65% to 75% ACN – 4 min, 75% to 90% ACN - 4 min, for a total of 33 min).

Both heated electrospray ionization (HESI) and atmospheric chemical ionization (APCI) were used in positive and negative modes for the ionization of products. HESI settings were: spray voltage 3.8 kV, vaporizer temperature of

150°C, capillary temperature 200°C, sheath gas flow of 8 arbitrary units (a.u.), auxiliary gas flow of 1 a.u., sweep gas flow of 0 a.u.. In APCI, settings were: corona discharge current of 3µA, spray voltage 3.8 kV, vaporizer temperature of 150°C, capillary temperature of 200°C, sheath gas flow of 8 a.u., auxiliary gas flow of 1 a.u., sweep gas flow of 0 a.u.,. In order to avoid transmission and detection effects of ions depending on their mass inside the C-Trap (Hecht et al., 2019), acquisitions with three mass ranges were performed (m/z 50-750; m/z 150-750; m/z 300-750). The upper limit of m/z 750 was chosen because of the absence of a signal beyond this value. It was shown that no significant oxidation occurred in the HESI and APCI ion sources by injecting a limonene-ACN mixture (Fig. S1). The optimization of the Orbitrap ionization parameters in HESI and APCI did not show any clustering phenomenon for these two monoterpene isomers. The parameters evaluated were: injection source - capillary distance, vaporization and capillary temperatures, applied difference of potential, injected volume, flow rate of nitrogen in the ionization source. Positive and negative HESI mass calibrations were performed using Pierce™ calibration mixtures (Thermo Scientific). Chemical compounds with relative intensity less than 1 ppm to the highest MS signal in the mass spectrum were not considered. Nevertheless, it should be considered that some of the molecules presented in this study could result from our experimental conditions (continuous flow reactor, reagent concentration, temperature, reaction time) and to some extent from our acquisition conditions, different from those in the previous studies (Deng et al., 2021;Quéléver et al., 2019;Meusinger et al., 2017;Krechmer et al., 2016;Tomaz et al., 2021;Fang et al., 2017;Witkowski and Gierczak, 2017;Jokinen et al., 2015;Nørgaard et al., 2013;Bateman et al., 2009;Walser et al., 2008;Warscheid and Hoffmann, 2001;Hammes et al., 2019;Kundu et al., 2012). Operating with a continuous flow reactor, at elevated temperature, and high initial concentration of reagents allows the formation of combustion-relevant products, which does not exclude their possible formation under atmospheric conditions. To assess the formation of products containing OOH and C=O groups, as in previous works (Belhadj et al., 2021a;Belhadj et al., 2021b), H/D exchange with D_2O and 2,4-dinitrophenyl hydrazine derivation were used, respectively.

3 Data Processing

High resolution mass spectrometry (HR-MS) generates large datasets which are difficult to fully analyze by sequential methods. When the study requires the processing of several thousands of molecules, the use of statistical tools and graphical representation means becomes necessary. In this study, we have chosen to use the van Krevelen diagram (Van Krevelen, 1950) by adding an additional dimension, the double bond equivalent (DBE). The DBE number represents the sum of unsaturation and rings present in a chemical compound (Melendez-Perez et al., 2016). The interest of this type of representation is to be able to identify more easily the clusters (increase of the DBE number at constant O/C and H/C ratios)

$$DBE = 1 + C - H/2$$

This number is independent of the number of O-atoms, but changes with the number of hydrogen atoms. Decimal values of this number, which correspond to an odd number of hydrogen atoms, were not considered in this study. Then, the superpositions of points (and therefore of chemical formulas) in the O/C vs. H/C space are suppressed. The oxidation state of carbon (OSc) provides a measure of the degree of oxidation of chemical compounds (Kroll et al., 2011). This provides a framework for describing the chemistry of organic species. It is defined by the following equation:

$$OSc \approx 2\ O/C - H/C$$

4 Results and discussion

We studied the oxidation of α-pinene and limonene ($C_{10}H_{16}$) at 590 K, under atmospheric pressure, with a residence time of 2 s, and a fuel concentration of 1%. Under these conditions, the formation of peroxides by autoxidation at low temperature should be efficient (Belhadj et al., 2021c), even though the conversion of the fuels remains moderate.

4.1 Characterization of ionization sources

First, we have studied the impact of APCI and HESI sources, in positive and negative modes, on the chemical formulas detected. The HESI and APCI sources in positive and negative mode were used and their operating parameters were varied, i.e., temperature, gas flow and accelerating voltage (see Section 2). For each polarity, only ions composed of carbon, hydrogen (even numbers) and oxygen were considered. Molecular duplicates inherent to mass range overlaps were excluded. By following these rules, we obtained a different number of ions depending on the ionization source and the polarity used. Table 1 shows the number of ions according to the experimental conditions and the discrimination rules.

Table 1. Number of ions detected for each source in positive and negative modes (by protonation or deprotonation, respectively)

Ionization source	α-Pinene		Limonene	
APCI	646 $(R+H)^+$	503 $(R–H)^-$	1321 $(R+H)^+$	1346 $(R–H)^-$
HESI	594 $(R+H)^+$	693 $(R–H)^-$	1017 $(R+H)^+$	1864 $(R–H)^-$

Each combination of ionization sources and polarity generated a set of chemical formulas. To make a meaningful comparison between the positive and negative ions data, the chemical formulas used were the precursors of the ions identified in the mass spectra. These sets have common data, but also specific chemical formulas. For a given ionization source, ~ 50% of the chemical formulas are observed whatever the ionization polarity, i.e., using both polarities one can capture between 30-50% more molecular species (since some of them are ionized under a single mode (+ or –) depending on their chemical structure). Utilizing both ionization polarities is helpful for identifying a larger quantity of species. The HESI source data were compared to the APCI data (Supplement, Tables S1 and S2), showing an increased number (20 to 30%) of chemical formulas detected by HESI. This increase is characterized by a better detection of negatively ionized species and those with a higher DBE. In order to evaluate further the interest for using these ionization sources, we compiled these data in Venn diagrams and proposed a visualization of these sets with a van Krevelen representation; we added the number of DBE in the third dimension (Supplement, Tables S1 and S2).

In positive ionization mode, independently of the ionization source and in addition to the common molecular formulas, we detected products with an O/C ratio < 0.2 whereas in the negative ionization mode, we detected molecular formulas with an O/C ratio > 0.5. In addition to these observations, we noted that HESI is more

appropriate for studying products with a large number of unsaturation (DBE > 5), which is probably related to the increase in the number of hydroperoxide and carboxyl groups along with the fact that a heated ionization source favors vaporization of low volatility compounds. Finally, for an optimal detection of the oxidation products, it is necessary to consider the transmission limits of the C-Trap. Here, we could increase by more than 60% the number of molecular formulas detected using several mass ranges for data acquisition (section 2.2). The most appropriate ionization polarity to be used is tied to chemical functions present in products to be detected. We could increase by 30 to 100% the number of chemical formulas detected by using both positive and negative ionization modes. Using HESI is consistent with previous findings indicating ESI is well suited for the ionization of acidic, polar, and heteroatom-containing chemicals (Kekäläinen et al., 2013). To illustrate the present results, HESI (–)-MS spectra are provided in the Supplement (Fig. S2).

4.2 Autoxidation products detected in a JSR

In order to compare the oxidation of α-pinene and limonene, we compiled the positive and negative ionization data obtained with APCI (Table S1) and HESI (Table S2) ionization sources to obtain a more exhaustive database. For the APCI and HESI sources, we distinguished three datasets, two of which are specific to the oxidation of α-pinene and limonene and one which is common to both isomers. In the following text, "only" will be used to describe the molecules specific to the oxidation of one of the isomeric terpenes. This common dataset represents more than 77% of the chemical formulas identified in the α-pinene oxidation samples detected with APCI. For limonene, for which the number of identified chemical formulas is greater, this common dataset represents over 93% of the chemical formulas detected after APCI ionization. In these two cases, the relatively low residence time (2 seconds) and the diversity of the chemical formulas obtained suggest that the oxidation of these two terpene isomers leads to ring opening, a phenomenon also observed in atmospheric chemistry (Berndt et al., 2016;Zhao et al., 2018;Iyer et al., 2021). Concerning the molecular formulas of products common to both isomers, Figure 1 shows that they are limited to compounds with 10 oxygen atoms or lower. This limit is linked to α-pinene whose oxidation beyond 10 oxygen atoms remains weak (less than 2% of the detected molecules for this terpene). In the case of limonene, the presence of an exocyclic double bond will increase, in a similar way to atmospheric chemistry (Kundu et al., 2012), the possibilities of oxidation and accretion. It remains however impossible, considering the size of the whole dataset and the diversity of the isomers, to formalize all the reaction mechanisms. Nevertheless, the formation of oxidized species can be described with the help of graphical tools. The number of oxygen atoms per molecule indicates that limonene oxidizes more than α-pinene (Fig. 1a). In the case of limonene, with a HESI source, chemicals with an oxygen number of up to 15 were detected. Most of the chemical formulas recorded had 8-10 O-atoms (Fig. 1c), whereas for α-pinene the products with >8 O-atoms were much less abundant (Fig. 1b). Moreover, for the products specific of limonene oxidation, this graph shows a distribution centered on 9 oxygen atoms with carbon skeletons probably resulting from accretion.

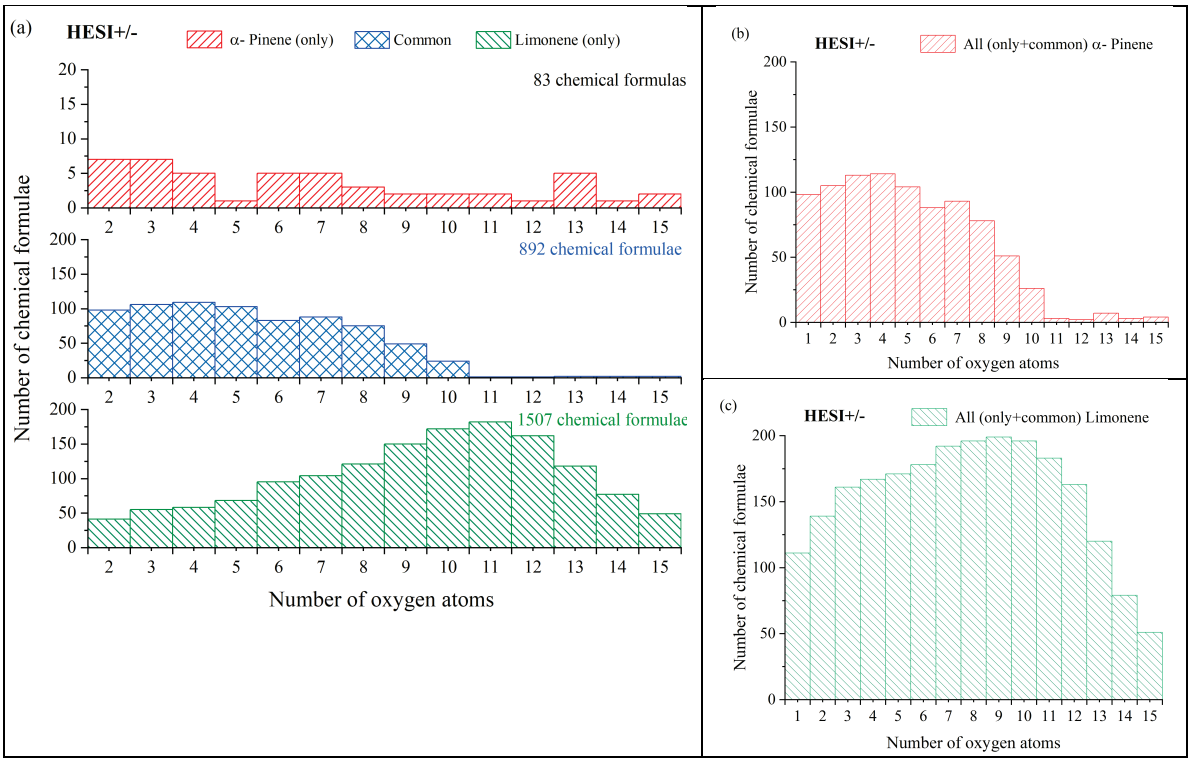

Figure 1: Distribution of α-pinene and limonene autoxidation products as a function of their oxygen content (ionization source: HESI, combined positive and negative modes data). (a) α-pinene and limonene HESI(+/-), (b) α-pinene HESI(+/–), (c) limonene HESI(+/–)

To verify this accretion hypothesis, we can plot the OSc as a function of the number of carbon atoms or the O/C ratio at fixed number of C-atoms (Fig. 2). Indeed, the presence of chemical compounds with 11 carbon atoms can be explained by an accretion phenomenon (Wang et al., 2021), but the advantage of this OSc vs. nC space representation (Kroll et al., 2011) is to allow studying this phenomenon on all the data. One can visualize the evolution of the molecular oxidation for each carbon skeleton and the formation of oligomers. Species that are unique to one of the isomers, or common to both are differentiated using different colors. In addition to the autoxidation represented by the vertical axis for a given number of carbon atoms (Fig. 2a), we observe mechanisms of fragmentation ($C_{<10}$), accretion and oligomerization ($C_{>10}$). These reaction mechanisms contribute to forming chemical classes according to their number of carbon atoms. The increase in the number of oxygen atoms, but also of carbon atoms will decrease products volatility. Following a classification proposed in the literature (Kroll et al., 2011), we distinguished four sets of products: low volatile oxidized organic aerosols (LV-OOA), semi-volatile oxidized organic aerosols (SV-OOA), biomass burning organic aerosols (BBOA) and water-soluble organic carbons (WSOC). In the OSc versus carbon number plot (Fig 2a), the vertical lines (at constant carbon number) are a first criterion for finding potential candidate products of autoxidation. Figure 2b shows, for a fixed number of carbon and hydrogen atoms and a difference of two oxygen atoms, the potential products of autoxidation connected by arrows whose color characterizes the oxygen parity. We can measure the extent of autoxidation for each carbon backbone in the OSc vs. O/C space. Using these criteria, we found that 73% of all chemical formulas are linked by a single difference of two oxygen atoms (which reflects an autoxidation mechanism). For the two terpenes, for which the initial carbon number is equal to 10, one can observe (Fig. 2b) two autoxidation routes with an even and odd number of oxygen atoms, respectively. This parity distinction is initially present for the two main

radicals, ROO˙ and RO˙ involved in autoxidation mechanisms. However, termination and propagation reactions will change the oxygen parity. Then, parity links between radicals and molecules are lost, which prevents interpretation of radical oxidation routes (Fig. 3). Figure 3 illustrates one of the reaction mechanisms (OH oxidation pathway) where oxygen parity changes through autoxidation. It should be noted that other reaction mechanisms can also change oxygen parity. In addition, the OH pathway in ozonolysis is not predominant. Figure 2 (b) illustrates the autoxidation routes between molecules resulting from a hydroperoxy radical reaction (arrows). In this case the oxygen parity is not modified and an OH radical is formed. HESI data showed an equivalent distribution of oxygen parities in molecular products (odd: 51%, even 49%) therefore confirming a lack of selectivity of the reaction mechanisms with respect to the oxygen parity of radicals.

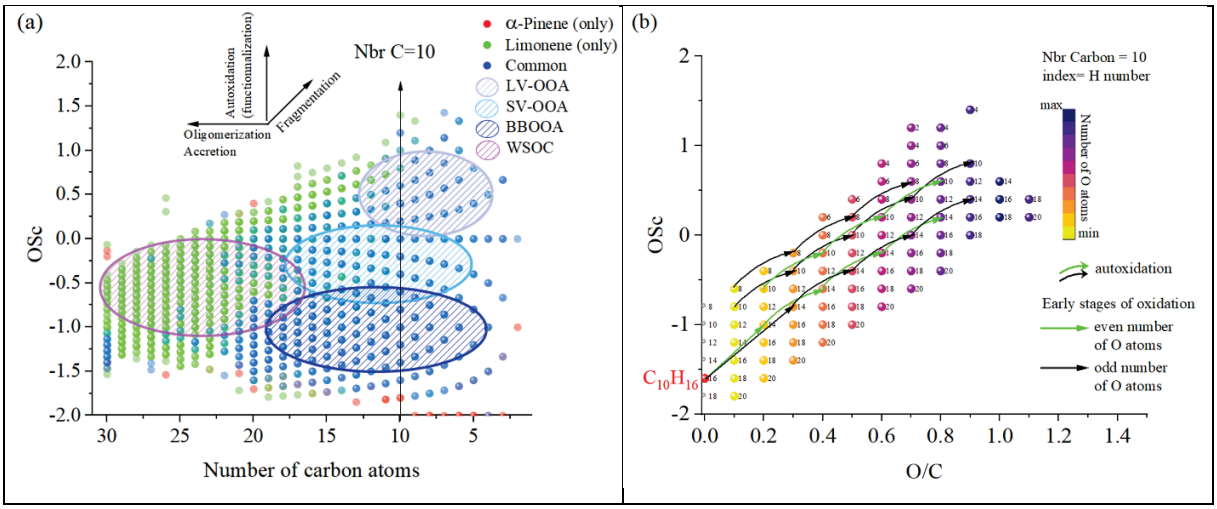

Figure 2: Overview of the distribution of limonene and α-pinene oxidation products observed in a JSR: (a) OSc versus carbon number in detected chemical formulas from APCI and HESI data. (b) OSc versus O/C atomic ratio for a carbon number of 10; index of the products: number of hydrogen atoms. Arrows indicate autoxidation from a $C_{10}H_{16}$ isomer, according to the oxygen parity in products

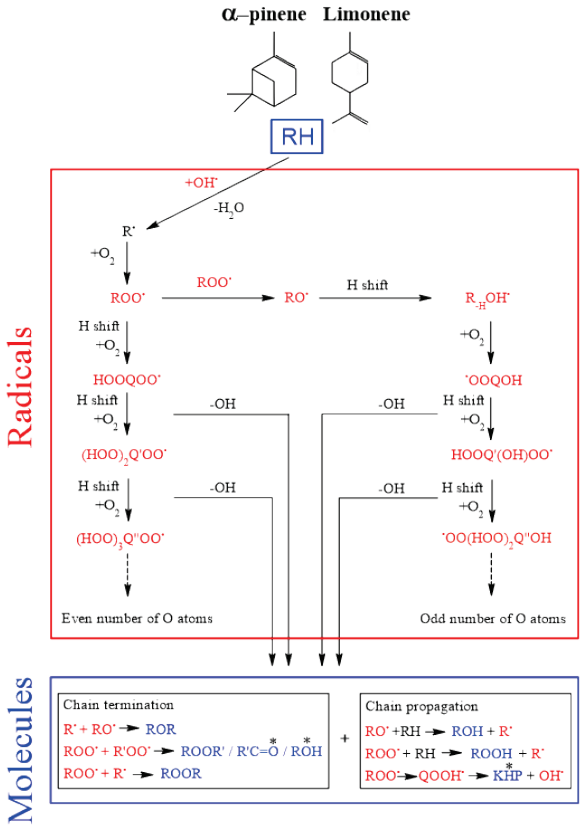

Figure 3: Accepted autoxidation reaction mechanisms in combustion (left) and in the atmosphere (left and right). * Indicates a change of oxygen atoms parity (Berndt et al., 2016).

4.3 Combustion versus atmospheric oxidation

4.3.1 Global analysis

We have explored potential chemical pathways related to autoxidation in the previous Section. For this purpose, we have performed experiments under cool flame conditions (590 K). This autoxidation mechanism is also present in atmospheric chemistry, but it is only recently that it has been found that this mechanism could be one of the main formation pathways for SOA (Savee et al., 2015;Crounse et al., 2013;Jokinen et al., 2014a;Iyer et al., 2021). Studies have described this mechanism in the case of atmospheric chemistry with the identification of radicals and molecular species (Tomaz et al., 2021). However, previous studies on the propagation of this reaction mechanism have mainly focused on the initial steps of autoxidation without screening all identified chemical formulas for potential autoxidation products. It is therefore useful to assess the proportion of possible autoxidation products among the total chemical species formed.

Here, we propose a new approach which consists in assessing a set of molecules mainly resulting from autoxidation against different sets of experimental studies related to atmospheric chemistry. The objective is to evaluate similarity of oxidation products formed under these conditions. For this purpose, we selected a HESI ionization source, better suited for detecting higher polarity oxidized molecules, as well as higher molecular weight products (detection of 96% of the total chemical formulas observed in autoxidation by APCI and HESI).

Among published atmospheric chemistry studies of terpenes oxidation, we have selected 15 studies presenting enough chemical products of oxidation, 4 for α-pinene and 11 for limonene. The data were acquired using different experimental procedures (methods of oxidation, techniques of characterization). Table 2 summarizes all the experimental parameters related to the selected studies. From that Table, one can note that few studies involved chromatographic analyzes (Tomaz, 2021; Witkowski an Gierczak, 2017; Warscheid and Hoffmann, 2001). The data are from the articles or files provided in the Supplement Tables S1 and S2. In these studies, oxidation was performed only by ozonolysis with different experimental conditions that gather the main methods described in the literature: ozonolysis, dark ozonolysis, ozonolysis with OH scavenger, ozonolysis with or without seed particles. We considered that the ionisation mode used in mass spectrometry did not modify the nature of the chemical species but only the relative detection of ions, depending on the type of ionization used, and the sensitivity of the instruments (Riva et al., 2019). The combination of data obtained using (+/-) HESI gives a rather complete picture of the autoxidation products.

First, we compared the data from ozonolysis studies of each terpene and identified similarities through Venn diagrams. For studies with two ionization sources, duplicate chemical formulas were removed. We selected the four most representative studies by the number of the chemical formulas detected. Then, we compared the set of chemical formulas identified after ozonolysis to those produced in low-temperature combustion, the objective being (i) to highlight similarities in terms of products generated by the two oxidation modes and (ii) to identify chemicals resulting from autoxidation.

365 **Table 2.** Experimental settings of 15 oxidation studies of two terpenes under atmospheric conditions and cool
366 flames (LC stands for liquid chromatography).

Reference	Oxidation mode	Sampling	Experimental setup	Concentrations of reactants	Ionization /source	Instrument	Chemical formulas	LC
α-Pinene								
Y. Deng et al. (2021)	Dark ozonolysis seed particles OH scavenger	online	Teflon bag; 0.7m^3	3.3±0.6 ncps ppbv^{-1} α -Pinene	ESI	ToF-MS	351	No
Quéléver et al. (2019)	Ozonolysis	online	Teflon bag 5 m^3	10 & 50 ppb α -Pinene	NO_3^- (CI)	CI-APi-TOF	68	No
Meusinger et al. (2017)	Dark Ozonolysis OH scavenger no seed particles	offline	Teflon bag 4.5 m^3	60 ppb α -Pinene	Proton transfer	PTR-MS-ToF	153	No
Krechmer et al. (2016)	Ozonolysis	offline	PAM Oxidation reactor	Field measurement	ESI (–) and NO_3^- (CI)	CI-IMS-ToF	43	No
This work	Cool-flame autoxidation	offline	Jet-stirred reactor 42 ml	1%, α -pinene No ozone	APCI(3kV) HESI (3kV)	Orbitrap® Q-Exactive	820 (APCI) 975 (HESI)	Yes
Limonene								
Krechmer et al. (2016)	Ozonolysis	offline	PAM Oxidation reactor	not specified	ESI (–) and NO_3^- (CI)	CI-IMS-ToF	63	No
Tomaz et al. (2021)	Ozonolysis	online	Flow tube reactor (18L)	45-227 ppb limonene	NO_3^- (CI) - Neg	Orbitrap® Q-Exactive	199	Yes
Fang et al. (2017)	OH-initiated photooxidation dark ozonolysis	online	Smog chamber	900–1500 ppb limonene	UV; 10 eV	Time-of-Flight (ToF)	17	No
Witkowski and Gierczak (2017)	Dark ozonolysis	offline	Flow reactor	2 ppm, limonene	ESI,4.5 kV	Triple quadrupole	12	Yes
(Jokinen et al., 2015)	Ozonolysis	online	Flow glass tube	1–10000 x10^9 molec.cm^{-3}, limonene	NO_3^- (CI)	Time-of-Flight (ToF)	11	No
Nørgaard et al. (2013)	Ozone (plasma)	online	direct on the support	850 ppb ozone 15-150 ppb limonene	plasma	Quadrupole time-of-flight (QToF)	29	No
Bateman et al. (2009)	Dark and UV radiations ozonolysis	offline	Teflon FEP reaction chamber	1 ppm ozone 1 ppm limonene	modified ESI (+/–)	LTQ-Orbitrap Hybrid Mass (ESI)	924	No
Walser et al. (2008)	Dark ozonolysis	offline	Teflon FEP reaction chamber	1-10 ppm ozone 10 ppm limonene	ESI (+/–); 4.5 kV	LTQ-Orbitrap Hybrid Mass (ESI)	465	No
Warscheid & Hoffmann (2001)	Ozonolysis	online	Smog chamber	300-500 ppb limonene	APCI; 3kV	Quadrupole ion trap mass	21	Yes
Hammes et al., (2019)	Dark ozonolysis	online	Flow reactor	15, 40, 150 ppb limonene	^{210} Po α acetate ions	HR-ToF-CIMS	20	No
Kundu et al. (2012)	Dark ozonolysis	offline	Teflon reaction chamber	250 ppb ozone 500 ppb limonene	ESI; 3.7 and 4 kV	LTQ FT Ultra, Thermo Sct (ESI)	1197	No
This work	Cool-flame autoxidation	offline	Jet-stirred reactor 42 ml	1%, limonene No ozone	APCI(3μA) HESI (3kV)	Orbitrap® Q-Exactive	1863(APCI) 2399(HESI)	Yes

367

368 For α-pinene oxidation, in the four selected studies 567 chemical formulas were detected, all polarities combined.
369 Only one study (Meusinger et al., 2017) was performed in positive ionization mode and none of the studies reported

data were obtained with two ionization modes (+/–). For the oxidation of limonene, the four selected studies identified 1434 chemical formulas. Among these studies, the experiments by Walser et al. were performed with both (+) and (–) ionisation modes. In contrast to the α-pinene case, the selected studies for limonene were performed with similar ionization sources, which probably contributed to increased data similarity (Walser et al., 2008). In the case of limonene oxidation, for which accretion is more important than for α-pinene, and for which a greater number of chemical formulas were identified, the similarities are more important (Jokinen et al., 2014b). These results are presented in Figure 4 where the ionization polarity used in each study is specified.

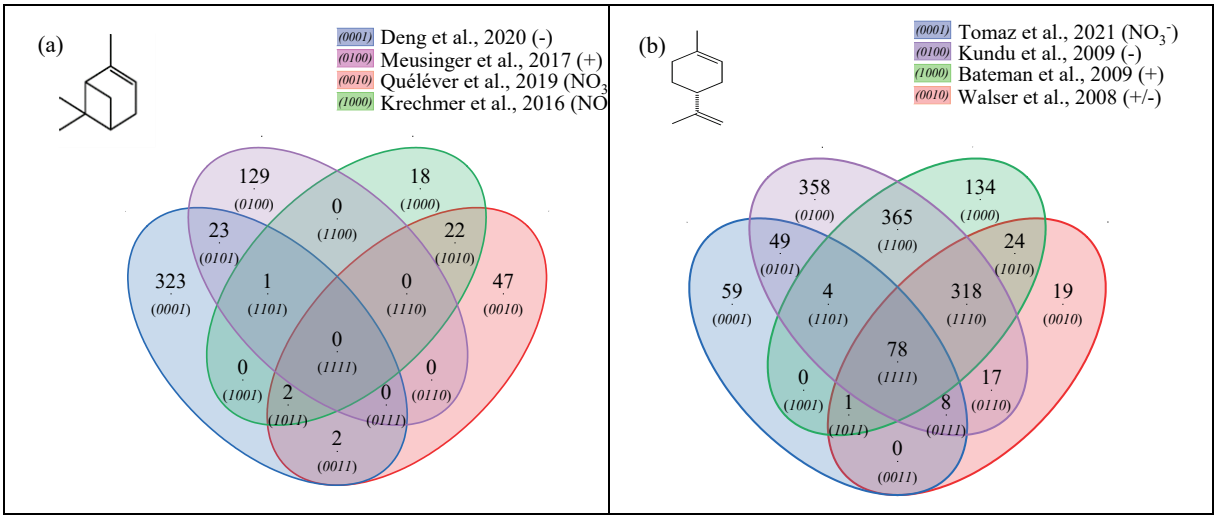

Figure 4: Venn diagrams for comparing the oxidation results from ozonolysis of (a) α-pinene and (b) limonene (see conditions in Table 1). Each digit indicates a study, the value of the digit characterizes the presence (value 1) or absence (0) common products detected in different studies, e.g., 23 chemical formulas (0101) (Fig. 4a) are common to the studies of Deng et al; (0001) and Meusinger et al. (0100)

For α-pinene, no chemical formula is common to all datasets. Different hypotheses can be offered to explain this result. Among them, the number of chemical formulas identified per study remains limited (a few dozen to several hundred) and these small datasets are sometimes restricted to specific mass ranges, e.g. C_{10} to C_{20} (Quéléver et al., 2019). In the case of studies carried out with an NO_3^- source, sensitive to HOMS, produced preferentially by autoxidation, we note that nearly 50% of the chemical formulas (10/22; (*1010*)) are linked by a simple difference of 2 oxygen atoms.

For limonene, 78 chemical formulas are common to the four studies selected here. In this data set, a large majority of chemical formulas show a similar relationship to autoxidation, i.e., a simple difference of two oxygen atoms: 62% (Tomaz et al., 2021), 54% (Walser et al., 2008), 69% (Kundu et al., 2012), 66% (Bateman et al., 2009) and 72% (this study). This result seems to indicate that autoxidation dominates.

One can then ask if reaction mechanisms common to atmospheric and combustion chemistry can generate, despite of radically different experimental conditions, a set of common chemical formulas and if in this common dataset, a common link, characteristic of autoxidation, is observable? To address that question, we compared all the previous results, for each of these terpenes to those obtained under the present combustion study. The comparisons were made using our HESI data. One should remember that the oxidation conditions in the JSR were chosen in order to maximize low-temperature autoxidation. Again, we used Venn diagrams to analyze these datasets

consisting of 1590 chemical formulas in the case of α-pinene and 5184 chemical formulas in the case of limonene. The results of these analyses are presented in Figure 5.

It turned out that for α-pinene, 301 chemical formulas and for limonene 871 chemical formulas were common to oxidation by ozonolysis (with or without scavenger) and combustion. This represents 31% of the chemical formulas for the ozonolysis of α-pinene and 36% for those of limonene ozonolysis. For α-pinene, the similarities compared to combustion are specific to each study: (Deng et al., 2021) 69% (243), (Meusinger et al., 2017) 46%, (71) (Quéléver et al., 2019) 7% (5), (Krechmer et al., 2016) 23% (10). Chemical formulas common to all studies were not identified. This lack of similarity may be due to a partial characterization of the chemical formulas, a weaker oxidation of α-pinene with an ionization mode less favorable to low molecular weights products.

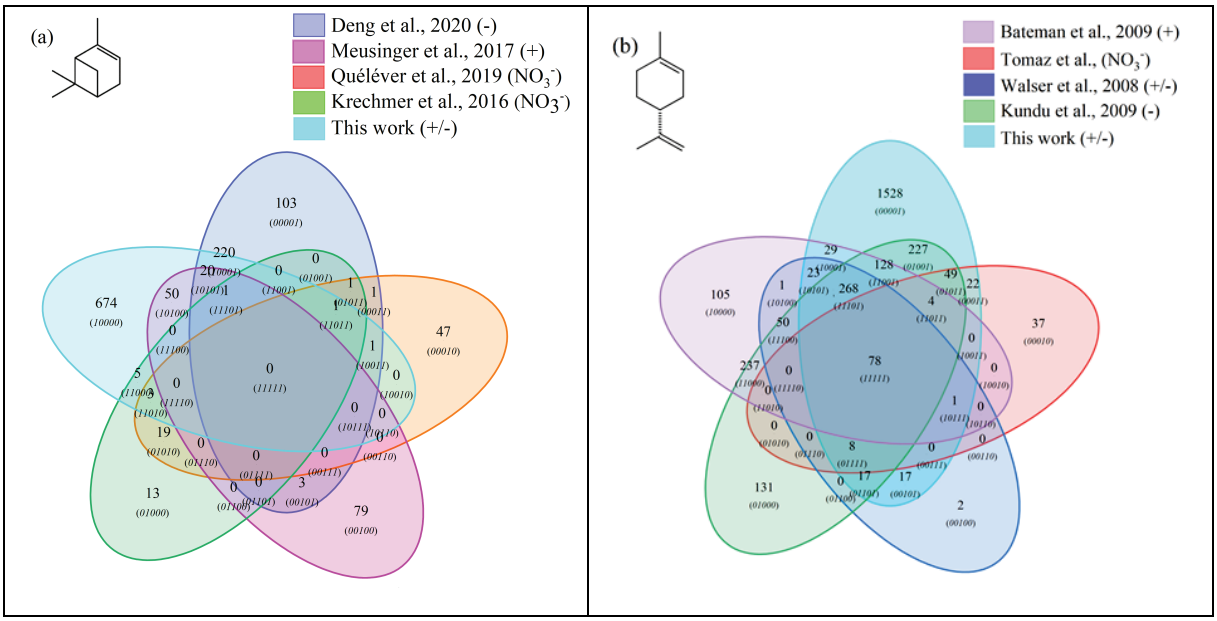

Figure 5: Venn diagrams comparing the oxidation results from ozonolysis and combustion of (a) α-pinene and (b) limonene (see conditions in Table 1).

For limonene, the similarities with combustion are more important and less spread out. They represent for the different studies: 65% (Kundu et al., 2012), 88% (Walser et al., 2008), 81% (Tomaz et al., 2021), and 57% (Bateman et al., 2009). Moreover, there is a common dataset of 78 chemical formulas which can derive from autoxidation mechanisms. Considering the very different experimental conditions, we must wonder about the impact of the double bonds in this similarity. In the case of limonene, we think their presence will indeed promote the formation of allylic radicals and then peroxide radicals (one of the motors of autoxidation). It is necessary to specify again that different reaction mechanisms can cause the observed similarities. However, the preponderance of autoxidation in so-called cool flame combustion is obvious, and in atmospheric chemistry, this reaction mechanism is competitive or dominates (Crounse et al., 2013;Jokinen et al., 2014a). If we search for an autoxidation link between these 78 chemical formulas, we observe that 45% of these chemical formulas meet this condition: difference of two oxygen atoms between formulas, at constant number of carbon and hydrogen atoms. More precisely, these molecules are centered in a van Krevelen diagram on the ratios O/C=0.6 and H/C=1.6, in the range $0.29 < O/C < 0.77$ and $1.33 < H/C < 1.8$. All oxidized molecules associated with this dataset are presented in Figure 6. The dispersion of the chemical formulas, far from being random, remains consistent with an autoxidation mechanism where the numbers of carbon and hydrogen atoms are constant.

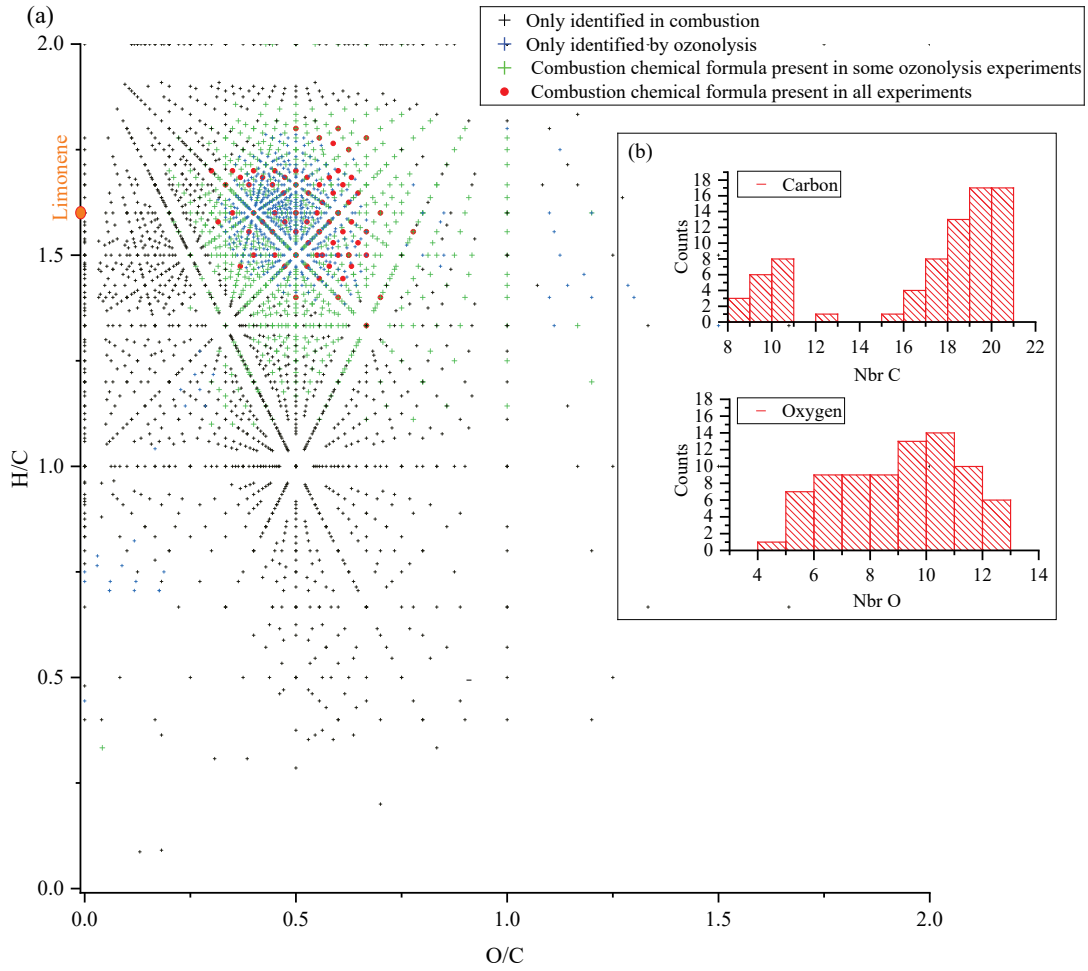

Figure 6: (a) Van Krevelen diagram showing specific and common chemical formulas detected after to oxidation of limonene by ozonolysis and combustion, insert (b): distributions of the number of carbon and oxygen atoms in the 78 chemical formulas common to all experiments.

A 3-D representation of all limonene oxidation data is given in Supplement (Fig. S3a) where DBE is used as third dimension. From that figure, one can note that products with higher DBE (DBE>10) are preferably formed under JSR conditions, i.e. at elevated temperature. A 2D representation (OSc vs DBE, Fig. S3b) completes this 3D view. The corresponding chemical formulas with DBE > 10 could correspond to carbonyls and / or cyclic ethers (•QOOH → carbonyl + alkene + OH and / or cyclic ether + OH•). Specificities and similarities of these two oxidation modes (ozonolysis/combustion) were further investigated by plotting the distribution of the number of oxygen atoms in detected chemical formulas (Fig. 7). Indeed, the distribution of the number of oxygen atoms allows, in addition to the Van Krevelen diagram, to provide some additional details on these two modes of oxidation. In ozonolysis, we observed the chemical formulas having the largest number of oxygen atoms. There, oxidation proceeds over a long reaction time where the phenomenon of aging appears through accretion or oligomerization. In combustion, the number of oxygen atoms remains limited to 18, with a lower number of detected chemical formulas compared to the case of ozonolysis. However, it is in combustion that we observed the highest O/C ratios, indicating the formation of the most oxidized products. This difference, however, does not affect the similarities between the chemical formulas detected in the two modes of oxidation. Finally, the analysis of the parities in oxygen atoms,

very similar for the three datasets, confirms that the reaction mechanisms presented in Figure 3 do not allow a simple link to be established between the oxygen parity of radicals and that of the detected molecular products.

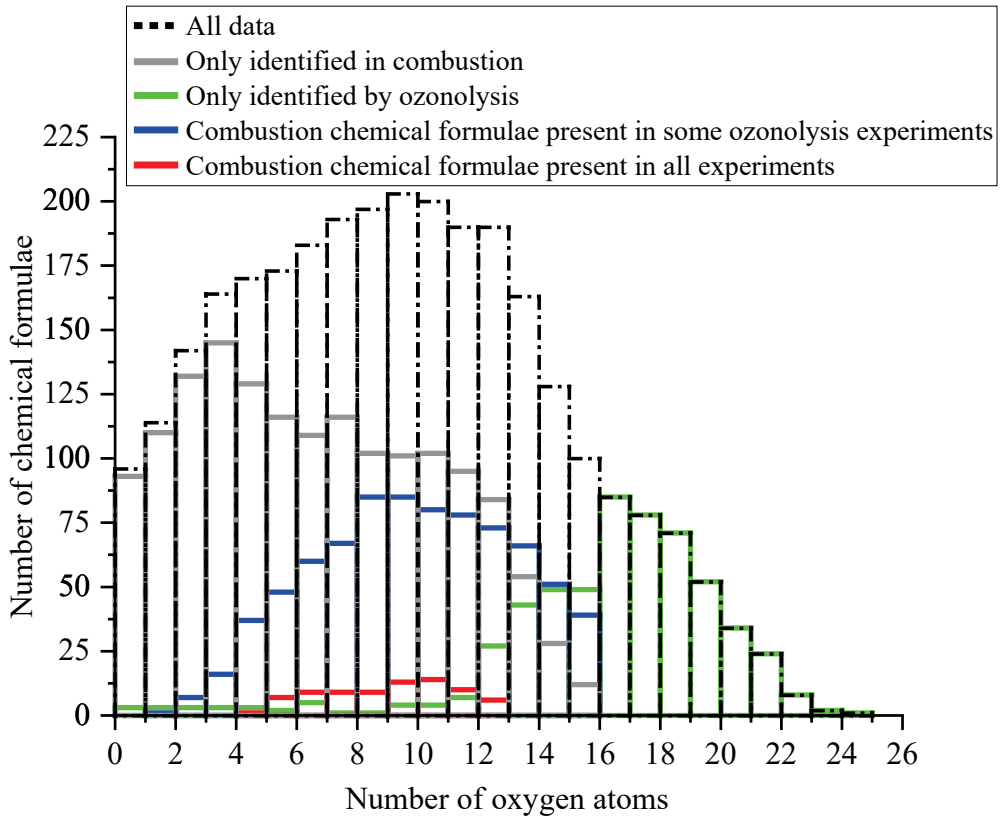

Figure 7: Oxygen number distribution for all the molecules identified for the oxidation of limonene: only in combustion, only in ozonolysis and common to both processes.

4.3.2 Identification of common isomers.

We identified a set of chemical formulas common to both atmospheric and combustion chemistries and suggested that this might result from an autoxidation mechanism. We identified several chemical formulas within this dataset that differ by two oxygen atoms on the same skeleton. Focusing on the early stages of limonene oxidation, there are several sequential two-oxygen additions to the chemical formulas $C_{10}H_{16}O_2$ and $C_{10}H_{16}O_3$ with the two oxygen parities described in Figure 3. Tables 3 presents the identified chemical formulas with information on the Venn index. The index for combustion is the rightmost (xxxx1).

Table 3. Sequential additions of two oxygens to the chemical formulas $C_{10}H_{16}O_2$ and $C_{10}H_{16}O_3$ present in the common set of 78 chemical formulas.

First stages of oxidation	1st addition	2nd addition	3rd addition	4th addition	5th addition
$C_{10}H_{16}O_2$ *(10101)*	$C_{10}H_{16}O_4$ *(11101)*	$C_{10}H_{16}O_6$ *(11111)*	$C_{10}H_{16}O_8$ *(01011)*	$C_{10}H_{16}O_{10}$ *(00011)*	$C_{10}H_{16}O_{12}$ *(00010)*
$C_{10}H_{16}O_3$ *(11101)*	$C_{10}H_{16}O_5$ *(11111)*	$C_{10}H_{16}O_7$ *(11111)*	$C_{10}H_{16}O_9$ *(01011)*	$C_{10}H_{16}O_{11}$ *(00010)*	

This result of sequential additions of two oxygens is also observed for other chemical formulas of this common dataset. Therefore, it questions the possibility that these two atmospheric and combustion chemistries develop autoxidation mechanisms with common isomers.

In order to verify this possibility, considering the differences between limonene and α-pinene, we analyzed by UHPLC-HRMS the chemical compounds $C_{10}H_{16}O_2$ for limonene and $C_{10}H_{16}O_3$ for α-pinene in the samples from the combustion experiments. For limonene and α-pinene, considering the availability of standards from suppliers, we selected limonoaldehyde and pinonic acid, respectively. These two isomers of $C_{10}H_{16}O_2$ and $C_{10}H_{16}O_3$ are among the most frequently reported products in atmospheric chemistry studies (Table 4). Our study shows same retention times for these standards and isomers detected in combustion samples (Fig S4). This result is more obvious for limonoaldehyde (11.5 min) than for pinonic acid (3.9 min). In addition, we detected the presence of -OH or -OOH groups by H/D exchange with D_2O for these two chemical formulas. Unfortunately, coelution did not fully allow exploiting MS/MS fragmentation carried out on the two chemical formulas, and to formally identify the two compounds. There is still a lot of characterization work to be done, but the hypothesis of common isomeric products formed through an autoxidation mechanism operating in atmospheric and low-temperature combustion conditions seems to be confirmed.

Table 4. Isomers of α-pinene and limonene oxidation reported in the literature.

	$C_{10}H_{16}O_2$		$C_{10}H_{16}O_3$	
α-pinene	Pinonaldehyde	(Fang et al., 2017)	Pinonic acid	(Fang et al., 2017;Ng et al., 2011;Meusinger et al., 2017)
	hydroxyketone	(Fang et al., 2017)	hydroxy pinonaldehydes	(Fang et al., 2017;Meusinger et al., 2017)
Limonene	limononaldehyde	(Fang et al., 2017;Walser et al., 2008;Bateman et al., 2009)	limononic acid	(Fang et al., 2017;Witkowski and Gierczak, 2017;Hammes et al., 2019;Walser et al., 2008;Bateman et al., 2009;Warscheid and Hoffmann, 2001)
	4-isopropenyl-methylhydroxy-2-oxocyclohexane	(Fang et al., 2017)	7-hydroxy-limononaldehyde	(Fang et al., 2017;Walser et al., 2008;Bateman et al., 2009;Meusinger et al., 2017)

5 Conclusion

The oxidation of limonene-oxygen-nitrogen and α-pinene-oxygen-nitrogen mixtures was carried out using a jet-stirred reactor at elevated temperature (590 K), a residence time of 2 s, and atmospheric pressure. The products were analyzed by liquid chromatography, flow injection, and soft ionization-high resolution mass spectrometry. H/D exchange and 2,4-dinitrophenyl hydrazine derivatization were used to assess the presence of OOH and C=O groups in products, respectively. We probed the effects of the type of ionization used in mass spectrometry analyses on the detection of oxidation products. Heated electrospray ionization (HESI +/–) and atmospheric pressure chemical ionization (APCI +/–) were used. A large dataset was obtained and compared with literature data obtained during the oxidation of limonene and α-pinene under simulated tropospheric and low-temperature oxidation conditions. This work showed a surprisingly similar set of chemical formulas of products, including oligomers, formed under the two rather different conditions, i.e., cool flames and simulated atmospheric oxidation. Data analysis involving van Krevelen diagrams, oxygen number distribution, oxidation state of carbon, and chemical relationship between molecules, indicated that a subset of chemical formulas is common to all experiments independently of experimental conditions. More than 35% of the chemical formulas detected in combustion chemistry experiments using a JSR have been detected in the studies carried out under atmospheric conditions.

Finally, we have outlined the existence of a substantial common dataset of autoxidation products. This result tends to show that autoxidation is indeed inducing similarity between atmospheric and combustion products. Detailed analysis of our data was performed by UHPLC-MS/MS of selected chemical formulas observed in the literature. Nevertheless, final identification was not possible due to coelutions.

The present JSR data could be useful to atmospheric chemists working in the field of wildfire and/or biomass burning induced air pollution. Considering that low-temperature oxidation (cool flame) products, i.e., VOCs, can be emitted from biomass burning, wildfires and engine exhausts, the present data should be of interest for the atmospheric chemists because they complement those obtained in atmospheric chemistry literature. It would be interesting to complement the atmospheric relevant data with MS^2 analyses of products and assessment of the presence of hydroperoxyl and carbonyl groups HOMs. Further MS^2 characterizations are also needed for the products observed in the present work. Finally, a study of the temperature dependence of products formation would be very useful, both under cool flame conditions and simulated atmospheric oxidation conditions.

Acknowledgements

The authors gratefully acknowledge funding from the Labex Caprysses (ANR-11-LABX-0006-01), the Labex Voltaire (ANR-10-LABX-100-01), CPER, and EFRD (PROMESTOCK and APPROPOR-e projects) and the French MESRI for a Ph.D. grant. We also thank (Tomaz et al., 2021) for sharing experimental data on limonene oxidation.

References

Bailey, H. C., and Norrish, R. G. W.: The oxidation of hexane in the cool-flame region, Proceedings of the Royal Society of London Series a-Mathematical and Physical Sciences, 212, 311-330, https://doi.org/10.1098/rspa.1952.0084, 1952.

Bateman, A. P., Nizkorodov, S. A., Laskin, J., and Laskin, A.: Time-resolved molecular characterization of limonene/ozone aerosol using high-resolution electrospray ionization mass spectrometry, Physical Chemistry Chemical Physics, 11, 7931-7942, https://doi.org/10.1039/B905288G, 2009.

Belhadj, N., Benoit, R., Dagaut, P., Lailliau, M., Serinyel, Z., Dayma, G., Khaled, F., Moreau, B., and Foucher, F.: Oxidation of di-n-butyl ether: Experimental characterization of low-temperature products in JSR and RCM, Combustion and Flame, 222, 133-144, https://doi.org/10.1016/j.combustflame.2020.08.037, 2020.

Belhadj, N., Benoit, R., Dagaut, P., and Lailliau, M.: Experimental characterization of n-heptane low-temperature oxidation products including keto-hydroperoxides and highly oxygenated organic molecules (HOMs), Combustion and Flame, 224, 83-93, https://doi.org/10.1016/j.combustflame.2020.10.021, 2021a.

Belhadj, N., Lailliau, M., Benoit, R., and Dagaut, P.: Towards a Comprehensive Characterization of the Low-Temperature Autoxidation of Di-n-Butyl Ether, Molecules, 26, 7174, 2021b.

Belhadj, N., Lailliau, M., Benoit, R., and Dagaut, P.: Experimental and kinetic modeling study of n-hexane oxidation. Detection of complex low-temperature products using high-resolution mass spectrometry, Combustion and Flame, 233, 111581, https://doi.org/10.1016/j.combustflame.2021.111581, 2021c.

Benoit, R., Belhadj, N., Lailliau, M., and Dagaut, P.: On the similarities and differences between the products of oxidation of hydrocarbons under simulated atmospheric conditions and cool flames, Atmos. Chem. Phys., 21, 7845-7862, https://doi.org/10.5194/acp-21-7845-2021, 2021.

Benson, S. W.: The kinetics and thermochemistry of chemical oxidation with application to combustion and flames, Progress in Energy and Combustion Science, 7, 125-134, https://doi.org/10.1016/0360-1285(81)90007-1, 1981.
Bernath, P., Boone, C., and Crouse, J.: Wildfire smoke destroys stratospheric ozone, Science, 375, 1292-1295, https://doi.org/10.1126/science.abm5611, 2022.
Berndt, T., Richters, S., Kaethner, R., Voigtländer, J., Stratmann, F., Sipilä, M., Kulmala, M., and Herrmann, H.: Gas-Phase Ozonolysis of Cycloalkenes: Formation of Highly Oxidized RO2 Radicals and Their Reactions with NO, NO2, SO2, and Other RO2 Radicals, The Journal of Physical Chemistry A, 119, 10336-10348, https://doi.org/10.1021/acs.jpca.5b07295, 2015.
Berndt, T., Richters, S., Jokinen, T., Hyttinen, N., Kurtén, T., Otkjær, R. V., Kjaergaard, H. G., Stratmann, F., Herrmann, H., Sipilä, M., Kulmala, M., and Ehn, M.: Hydroxyl radical-induced formation of highly oxidized organic compounds, Nat Commun, 7, 13677, https://doi.org/10.1038/ncomms13677, 2016.
Bianchi, F., Kurtén, T., Riva, M., Mohr, C., Rissanen, M. P., Roldin, P., Berndt, T., Crounse, J. D., Wennberg, P. O., Mentel, T. F., Wildt, J., Junninen, H., Jokinen, T., Kulmala, M., Worsnop, D. R., Thornton, J. A., Donahue, N., Kjaergaard, H. G., and Ehn, M.: Highly Oxygenated Organic Molecules (HOM) from Gas-Phase Autoxidation Involving Peroxy Radicals: A Key Contributor to Atmospheric Aerosol, Chemical Reviews, 119, 3472-3509, https://doi.org/10.1021/acs.chemrev.8b00395, 2019.
Burke, M., Driscoll, A., Heft-Neal, S., Xue, J., Burney, J., and Wara, M.: The changing risk and burden of wildfire in the United States, Proceedings of the National Academy of Sciences, 118, e2011048118, doi:10.1073/pnas.2011048118, 2021.
Camredon, M., Hamilton, J. F., Alam, M. S., Wyche, K. P., Carr, T., White, I. R., Monks, P. S., Rickard, A. R., and Bloss, W. J.: Distribution of gaseous and particulate organic composition during dark α-pinene ozonolysis, Atmos. Chem. Phys., https://doi.org/10, 2893-2917, https://doi.org/10.5194/acp-10-2893-2010, 2010.
Cox, R. A., and Cole, J. A.: Chemical aspects of the autoignition of hydrocarbon-air mixtures, Combust. Flame, 60, 109-123, https://doi.org/10.1016/0010-2180(85)90001-X, 1985.
Crounse, J. D., Nielsen, L. B., Jørgensen, S., Kjaergaard, H. G., and Wennberg, P. O.: Autoxidation of organic compounds in the atmosphere, J. Phys. Chem. Lett., 4, 3513, 2013.
Dagaut, P., Cathonnet, M., Rouan, J. P., Foulatier, R., Quilgars, A., Boettner, J. C., Gaillard, F., and James, H.: A jet-stirred reactor for kinetic studies of homogeneous gas-phase reactions at pressures up to ten atmospheres (≈1 MPa), Journal of Physics E: Scientific Instruments, 19, 207-209, https://doi.org/10.1088/0022-3735/19/3/009, 1986.
Dagaut, P., Cathonnet, M., Boetiner, J. C., and Gaillard, F.: Kinetic Modeling of Propane Oxidation, Combustion Science and Technology, 56, 23-63, https://doi.org/10.1080/00102208708947080, 1987.
Dagaut, P., Cathonnet, M., Boettner, J. C., and Gaillard, F.: Kinetic modeling of ethylene oxidation, Combustion and Flame, 71, 295-312, https://doi.org/10.1016/0010-2180(88)90065-X, 1988.
Deng, Y., Inomata, S., Sato, K., Ramasamy, S., Morino, Y., Enami, S., and Tanimoto, H.: Temperature and acidity dependence of secondary organic aerosol formation from α-pinene ozonolysis with a compact chamber system, Atmos. Chem. Phys., 21, 5983-6003, https://doi.org/10.5194/acp-21-5983-2021, 2021.
Ehn, M., Thornton, J. A., Kleist, E., Sipila, M., Junninen, H., Pullinen, I., Springer, M., Rubach, F., Tillmann, R., Lee, B., Lopez-Hilfiker, F., Andres, S., Acir, I. H., Rissanen, M., Jokinen, T., Schobesberger, S., Kangasluoma, J., Kontkanen, J., Nieminen, T., Kurten, T., Nielsen, L. B., Jorgensen, S., Kjaergaard, H. G., Canagaratna, M., Maso, M. D., Berndt, T., Petaja, T., Wahner, A., Kerminen, V. M., Kulmala, M., Worsnop, D. R., Wildt, J., and Mentel, T. F.: A large source of low-volatility secondary organic aerosol, Nature, 506, 476-479, https://doi.org/10.1038/nature13032, 2014.
Fang, W., Gong, L., and Sheng, L.: Online analysis of secondary organic aerosols from OH-initiated photooxidation and ozonolysis of α-pinene, β-pinene, Δ3-carene and d-limonene by thermal

584 desorption–photoionisation aerosol mass spectrometry, Environmental Chemistry, 14, 75-90,
585 https://doi.org/10.1071/EN16128, 2017.
586 Gilman, J. B., Lerner, B. M., Kuster, W. C., Goldan, P. D., Warneke, C., Veres, P. R., Roberts, J. M., de
587 Gouw, J. A., Burling, I. R., and Yokelson, R. J.: Biomass burning emissions and potential air quality
588 impacts of volatile organic compounds and other trace gases from fuels common in the US,
589 Atmos. Chem. Phys., 15, 13915-13938, https://doi.org/10.5194/acp-15-13915-2015, 2015.
590 Hammes, J., Lutz, A., Mentel, T., Faxon, C., and Hallquist, M.: Carboxylic acids from limonene
591 oxidation by ozone and hydroxyl radicals: insights into mechanisms derived using a FIGAERO-
592 CIMS, Atmos. Chem. Phys., 19, 13037-13052, https://doi.org/10.5194/acp-19-13037-2019, 2019.
593 Harvey, B. G., Wright, M. E., and Quintana, R. L.: High-Density Renewable Fuels Based on the
594 Selective Dimerization of Pinenes, Energy Fuels, 24, 267-273, https://doi.org/10.1021/ef900799c,
595 2010.
596 Harvey, B. G., Merriman, W. W., and Koontz, T. A.: High-Density Renewable Diesel and Jet Fuels
597 Prepared from Multicyclic Sesquiterpanes and a 1-Hexene-Derived Synthetic Paraffinic Kerosene,
598 Energy Fuels, 29, 2431-2436, https://doi.org/10.1021/ef5027746, 2015.
599 Hatch, L. E., Jen, C. N., Kreisberg, N. M., Selimovic, V., Yokelson, R. J., Stamatis, C., York, R. A., Foster,
600 D., Stephens, S. L., Goldstein, A. H., and Barsanti, K. C.: Highly Speciated Measurements of
601 Terpenoids Emitted from Laboratory and Mixed-Conifer Forest Prescribed Fires, Environmental
602 Science & Technology, 53, 9418-9428, https://doi.org/10.1021/acs.est.9b02612, 2019.
603 Hecht, E. S., Scigelova, M., Eliuk, S., and Makarov, A.: Fundamentals and Advances of Orbitrap Mass
604 Spectrometry, Encyclopedia of Analytical Chemistry, 1-40,
605 https://doi.org/10.1002/9780470027318.a9309.pub2, 2019.
606 Hu, Y., Fernandez-Anez, N., Smith, T. E. L., and Rein, G.: Review of emissions from smouldering peat
607 fires and their contribution to regional haze episodes, International Journal of Wildland Fire, 27,
608 293-312, https://doi.org/10.1071/WF17084, 2018.
609 Huang, W., Saathoff, H., Pajunoja, A., Shen, X., Naumann, K. H., Wagner, R., Virtanen, A., Leisner, T.,
610 and Mohr, C.: α-Pinene secondary organic aerosol at low temperature: chemical composition and
611 implications for particle viscosity, Atmos. Chem. Phys., 18, 2883-2898,
612 https://doi.org/10.5194/acp-18-2883-2018, 2018.
613 Iyer, S., Rissanen, M. P., Valiev, R., Barua, S., Krechmer, J. E., Thornton, J., Ehn, M., and Kurtén, T.:
614 Molecular mechanism for rapid autoxidation in α-pinene ozonolysis, Nature Communications, 12,
615 878, https://doi.org/10.1038/s41467-021-21172-w, 2021.
616 Jokinen, T., Sipilä, M., Richters, S., Kerminen, V.-M., Paasonen, P., Stratmann, F., Worsnop, D.,
617 Kulmala, M., Ehn, M., Herrmann, H., and Berndt, T.: Rapid Autoxidation Forms Highly Oxidized
618 RO2 Radicals in the Atmosphere, Angewandte Chemie International Edition, 53, 14596-14600,
619 https://doi.org/10.1002/anie.201408566, 2014a.
620 Jokinen, T., Sipila, M., Richters, S., Kerminen, V. M., Paasonen, P., Stratmann, F., Worsnop, D.,
621 Kulmala, M., Ehn, M., and Herrmann, H.: Rapid autoxidation forms highly oxidized RO2 radicals in
622 the atmosphere, Angew. Chem., Int. Ed., 53, 14596, 2014b.
623 Jokinen, T., Berndt, T., Makkonen, R., Kerminen, V.-M., Junninen, H., Paasonen, P., Stratmann, F.,
624 Herrmann, H., Guenther, A. B., Worsnop, D. R., Kulmala, M., Ehn, M., and Sipilä, M.: Production of
625 extremely low volatile organic compounds from biogenic emissions: Measured yields and
626 atmospheric implications, Proceedings of the National Academy of Sciences, 112, 7123-7128,
627 https://doi.org/10.1073/pnas.1423977112, 2015.
628 Kekäläinen, T., Pakarinen, J. M. H., Wickström, K., Lobodin, V. V., McKenna, A. M., and Jänis, J.:
629 Compositional Analysis of Oil Residues by Ultrahigh-Resolution Fourier Transform Ion Cyclotron
630 Resonance Mass Spectrometry, Energy Fuels, 27, 2002-2009, https://doi.org/10.1021/ef301762v,
631 2013.
632 Khaykin, S., Legras, B., Bucci, S., Sellitto, P., Isaksen, L., Tencé, F., Bekki, S., Bourassa, A., Rieger, L.,
633 Zawada, D., Jumelet, J., and Godin-Beekmann, S.: The 2019/20 Australian wildfires generated a
634 persistent smoke-charged vortex rising up to 35 km altitude, Communications Earth &
635 Environment, 1, 22, https://doi.org/10.1038/s43247-020-00022-5, 2020.

636 Kobziar, L. N., Pingree, M. R. A., Larson, H., Dreaden, T. J., Green, S., and Smith, J. A.:
637 Pyroaerobiology: the aerosolization and transport of viable microbial life by wildland fire,
638 Ecosphere, 9, e02507, https://doi.org/10.1002/ecs2.2507, 2018.
639 Korcek, S., Ingold, K. U., Chenier, J. H. B., and Howard, J. A.: Absolute rate constants for hydrocarbon
640 autoxidation .21. Activation-energies for propagation and correlation of propagation rate
641 constants with carbon-hydrogen bond strengths, Canadian Journal of Chemistry, 50, 2285-&,
642 https://doi.org/10.1139/v72-365, 1972.
643 Kourtchev, I., Doussin, J. F., Giorio, C., Mahon, B., Wilson, E. M., Maurin, N., Pangui, E., Venables, D.
644 S., Wenger, J. C., and Kalberer, M.: Molecular Composition of Fresh and Aged Secondary Organic
645 Aerosol from a Mixture of Biogenic Volatile Compounds: A High-Resolution Mass Spectrometry
646 Study, Atmos. Chem. Phys., 15, 5683, 2015.
647 Krechmer, J. E., Groessl, M., Zhang, X., Junninen, H., Massoli, P., Lambe, A. T., Kimmel, J. R., Cubison,
648 M. J., Graf, S., Lin, Y. H., Budisulistiorini, S. H., Zhang, H., Surratt, J. D., Knochenmuss, R., Jayne, J.
649 T., Worsnop, D. R., Jimenez, J. L., and Canagaratna, M. R.: Ion mobility spectrometry–mass
650 spectrometry (IMS–MS) for on- and offline analysis of atmospheric gas and aerosol species,
651 Atmos. Meas. Tech., 9, 3245-3262, https://doi.org/10.5194/amt-9-3245-2016, 2016.
652 Kristensen, K., Watne, Å. K., Hammes, J., Lutz, A., Petäjä, T., Hallquist, M., Bilde, M., and Glasius, M.:
653 High-Molecular Weight Dimer Esters Are Major Products in Aerosols from α-Pinene Ozonolysis
654 and the Boreal Forest, Environmental Science & Technology Letters, 3, 280-285,
655 https://doi.org/10.1021/acs.estlett.6b00152, 2016.
656 Kroll, J. H., Donahue, N. M., Jimenez, J. L., Kessler, S. H., Canagaratna, M. R., Wilson, K. R., Altieri, K.
657 E., Mazzoleni, L. R., Wozniak, A. S., Bluhm, H., Mysak, E. R., Smith, J. D., Kolb, C. E., and Worsnop,
658 D. R.: Carbon oxidation state as a metric for describing the chemistry of atmospheric organic
659 aerosol, Nature Chemistry, 3, 133-139, https://doi.org/10.1038/nchem.948, 2011.
660 Kundu, S., Fisseha, R., Putman, A. L., Rahn, T. A., and Mazzoleni, L. R.: High molecular weight SOA
661 formation during limonene ozonolysis: insights from ultrahigh-resolution FT-ICR mass
662 spectrometry characterization, Atmos. Chem. Phys., 12, 5523-5536, https://doi.org/10.5194/acp-
663 12-5523-2012, 2012.
664 Kurtén, T., Rissanen, M. P., Mackeprang, K., Thornton, J. A., Hyttinen, N., Jørgensen, S., Ehn, M., and
665 Kjaergaard, H. G.: Computational Study of Hydrogen Shifts and Ring-Opening Mechanisms in α-
666 Pinene Ozonolysis Products, The Journal of Physical Chemistry A, 119, 11366-11375,
667 https://doi.org/10.1021/acs.jpca.5b08948, 2015.
668 Melendez-Perez, J. J., Martínez-Mejia, M. J., and Eberlin, M. N.: A reformulated aromaticity index
669 equation under consideration for non-aromatic and non-condensed aromatic cyclic carbonyl
670 compounds, Organic Geochemistry, 95, 29-33,
671 https://doi.org/10.1016/j.orggeochem.2016.02.002, 2016.
672 Meusinger, C., Dusek, U., King, S. M., Holzinger, R., Rosenørn, T., Sperlich, P., Julien, M., Remaud, G.
673 S., Bilde, M., Röckmann, T., and Johnson, M. S.: Chemical and isotopic composition of secondary
674 organic aerosol generated by α-pinene ozonolysis, Atmos. Chem. Phys., 17, 6373-6391,
675 https://doi.org/10.5194/acp-17-6373-2017, 2017.
676 Mewalal, R., Rai, D. K., Kainer, D., Chen, F., Külheim, C., Peter, G. F., and Tuskan, G. A.: Plant-Derived
677 Terpenes: A Feedstock for Specialty Biofuels, Trends Biotechnol., 35, 227-240,
678 https://doi.org/10.1016/j.tibtech.2016.08.003, 2017.
679 Ng, N. L., Canagaratna, M. R., Jimenez, J. L., Chhabra, P. S., Seinfeld, J. H., and Worsnop, D. R.:
680 Changes in organic aerosol composition with aging inferred from aerosol mass spectra, Atmos.
681 Chem. Phys., 11, 6465-6474, https://doi.org/10.5194/acp-11-6465-2011, 2011.
682 Nørgaard, A. W., Vibenholt, A., Benassi, M., Clausen, P. A., and Wolkoff, P.: Study of Ozone-Initiated
683 Limonene Reaction Products by Low Temperature Plasma Ionization Mass Spectrometry, Journal
684 of The American Society for Mass Spectrometry, 24, https://doi.org/1090-1096, 10.1007/s13361-
685 013-0648-3, 2013.
686 Nozière, B., Kalberer, M., Claeys, M., Allan, J., D'Anna, B., Decesari, S., Finessi, E., Glasius, M., Grgić, I.,
687 Hamilton, J. F., Hoffmann, T., Iinuma, Y., Jaoui, M., Kahnt, A., Kampf, C. J., Kourtchev, I.,

688 Maenhaut, W., Marsden, N., Saarikoski, S., Schnelle-Kreis, J., Surratt, J. D., Szidat, S., Szmigielski,
689 R., and Wisthaler, A.: The Molecular Identification of Organic Compounds in the Atmosphere:
690 State of the Art and Challenges, Chemical Reviews, 115, 3919-3983,
691 https://doi.org/10.1021/cr5003485, 2015.
692 Otkjær, R. V., Jakobsen, H. H., Tram, C. M., and Kjaergaard, H. G.: Calculated Hydrogen Shift Rate
693 Constants in Substituted Alkyl Peroxy Radicals, The Journal of Physical Chemistry A, 122, 8665-
694 8673, https://doi.org/10.1021/acs.jpca.8b06223, 2018.
695 Popovicheva, O. B., Engling, G., Ku, I. T., Timofeev, M. A., and Shonija, N. K.: Aerosol Emissions from
696 Long-lasting Smoldering of Boreal Peatlands: Chemical Composition, Markers, and Microstructure,
697 Aerosol and Air Quality Research, 19, 484-503, https://doi.org/10.4209/aaqr.2018.08.0302, 2019.
698 Prichard, S. J., O'Neill, S. M., Eagle, P., Andreu, A. G., Drye, B., Dubowy, J., Urbanski, S., and Strand, T.
699 M.: Wildland fire emission factors in North America: synthesis of existing data, measurement
700 needs and management applications, International Journal of Wildland Fire, 29, 132-147,
701 https://doi.org/10.1071/WF19066, 2020.
702 Quéléver, L. L. J., Kristensen, K., Normann Jensen, L., Rosati, B., Teiwes, R., Daellenbach, K. R.,
703 Peräkylä, O., Roldin, P., Bossi, R., Pedersen, H. B., Glasius, M., Bilde, M., and Ehn, M.: Effect of
704 temperature on the formation of highly oxygenated organic molecules (HOMs) from alpha-pinene
705 ozonolysis, Atmos. Chem. Phys., 19, 7609-7625, https://doi.org/10.5194/acp-19-7609-2019, 2019.
706 Riva, M., Rantala, P., Krechmer, J. E., Peräkylä, O., Zhang, Y., Heikkinen, L., Garmash, O., Yan, C.,
707 Kulmala, M., Worsnop, D., and Ehn, M.: Evaluating the performance of five different chemical
708 ionization techniques for detecting gaseous oxygenated organic species, Atmos. Meas. Tech., 12,
709 2403-2421, https://doi.org/10.5194/amt-12-2403-2019, 2019.
710 Savee, J. D., Papajak, E., Rotavera, B., Huang, H., Eskola, A. J., Welz, O., Sheps, L., Taatjes, C. A., Zádor,
711 J., and Osborn, D. L.: Carbon radicals. Direct observation and kinetics of a hydroperoxyalkyl radical
712 (QOOH), Science, 347, 643-646, https://doi.org/10.1126/science.aaa1495, 2015.
713 Schneider, E., Czech, H., Popovicheva, O., Lütdke, H., Schnelle-Kreis, J., Khodzher, T., Rüger, C. P., and
714 Zimmermann, R.: Molecular Characterization of Water-Soluble Aerosol Particle Extracts by
715 Ultrahigh-Resolution Mass Spectrometry: Observation of Industrial Emissions and an
716 Atmospherically Aged Wildfire Plume at Lake Baikal, ACS Earth and Space Chemistry, 6, 1095-
717 1107, https://doi.org/10.1021/acsearthspacechem.2c00017, 2022.
718 Seinfeld, J. H., and Pandis, S. N.: Atmospheric Chemistry and Physics: From Air Pollution to Climate
719 Change, 2nd ed., Wiley-Interscience, Hoboken, NJ, 1232 pp., 2006.
720 Smith, J. S., Laskin, A., and Laskin, J.: Molecular Characterization of Biomass Burning Aerosols Using
721 High-Resolution Mass Spectrometry, Analytical Chemistry, 81, 1512-1521,
722 https://doi.org/10.1021/ac8020664, 2009.
723 Tomaz, S., Wang, D., Zabalegui, N., Li, D., Lamkaddam, H., Bachmeier, F., Vogel, A., Monge, M. E.,
724 Perrier, S., Baltensperger, U., George, C., Rissanen, M., Ehn, M., El Haddad, I., and Riva, M.:
725 Structures and reactivity of peroxy radicals and dimeric products revealed by online tandem mass
726 spectrometry, Nature Communications, 12, 300, https://doi.org/10.1038/s41467-020-20532-2,
727 2021.
728 Tröstl, J., Chuang, W. K., Gordon, H., Heinritzi, M., Yan, C., Molteni, U., Ahlm, L., Frege, C., Bianchi, F.,
729 Wagner, R., Simon, M., Lehtipalo, K., Williamson, C., Craven, J. S., Duplissy, J., Adamov, A.,
730 Almeida, J., Bernhammer, A.-K., Breitenlechner, M., Brilke, S., Dias, A., Ehrhart, S., Flagan, R. C.,
731 Franchin, A., Fuchs, C., Guida, R., Gysel, M., Hansel, A., Hoyle, C. R., Jokinen, T., Junninen, H.,
732 Kangasluoma, J., Keskinen, H., Kim, J., Krapf, M., Kürten, A., Laaksonen, A., Lawler, M., Leiminger,
733 M., Mathot, S., Möhler, O., Nieminen, T., Onnela, A., Petäjä, T., Piel, F. M., Miettinen, P., Rissanen,
734 M. P., Rondo, L., Sarnela, N., Schobesberger, S., Sengupta, K., Sipilä, M., Smith, J. N., Steiner, G.,
735 Tomè, A., Virtanen, A., Wagner, A. C., Weingartner, E., Wimmer, D., Winkler, P. M., Ye, P., Carslaw,
736 K. S., Curtius, J., Dommen, J., Kirkby, J., Kulmala, M., Riipinen, I., Worsnop, D. R., Donahue, N. M.,
737 and Baltensperger, U.: The role of low-volatility organic compounds in initial particle growth in the
738 atmosphere, Nature, 533, 527-531, https://doi.org/10.1038/nature18271, 2016.

Van Krevelen, D. W.: Graphical-statistical method for the study of structure and reaction processes of coal, Fuel, 29, 269-284, 1950.

Vereecken, L., Müller, J. F., and Peeters, J.: Low-volatility poly-oxygenates in the OH-initiated atmospheric oxidation of α-pinene: impact of non-traditional peroxyl radical chemistry, Physical Chemistry Chemical Physics, 9, 5241-5248, https://doi.org/10.1039/B708023A, 2007.

Walser, M. L., Desyaterik, Y., Laskin, J., Laskin, A., and Nizkorodov, S. A.: High-resolution mass spectrometric analysis of secondary organic aerosol produced by ozonation of limonene, Physical Chemistry Chemical Physics, 10, 1009-1022, https://doi.org/10.1039/B712620D, 2008.

Wang, Z., Popolan-Vaida, D. M., Chen, B., Moshammer, K., Mohamed, S. Y., Wang, H., Sioud, S., Raji, M. A., Kohse-Höinghaus, K., Hansen, N., Dagaut, P., Leone, S. R., and Sarathy, S. M.: Unraveling the structure and chemical mechanisms of highly oxygenated intermediates in oxidation of organic compounds, Proceedings of the National Academy of Sciences, 114, 13102-13107, https://doi.org/10.1073/pnas.1707564114, 2017.

Wang, Z., Chen, B., Moshammer, K., Popolan-Vaida, D. M., Sioud, S., Shankar, V. S. B., Vuilleumier, D., Tao, T., Ruwe, L., Bräuer, E., Hansen, N., Dagaut, P., Kohse-Höinghaus, K., Raji, M. A., and Sarathy, S. M.: n-Heptane cool flame chemistry: Unraveling intermediate species measured in a stirred reactor and motored engine, Combustion and Flame, 187, 199-216, https://doi.org/10.1016/j.combustflame.2017.09.003, 2018.

Wang, Z., Ehn, M., Rissanen, M. P., Garmash, O., Quéléver, L., Xing, L., Monge Palacios, M., Rantala, P., Donahue, N. M., Berndt, T., and Sarathy, M.: - Efficient alkane oxidation under combustion engine and atmospheric conditions, Communications Chemistry, 4, 18, https://doi.org/10.1038/s42004-020-00445-3, 2021.

Warscheid, B., and Hoffmann, T.: Structural elucidation of monoterpene oxidation products by ion trap fragmentation using on-line atmospheric pressure chemical ionisation mass spectrometry in the negative ion mode, Rapid Communications in Mass Spectrometry, 15, 2259-2272, https://doi.org/10.1002/rcm.504, 2001.

Witkowski, B., and Gierczak, T.: Characterization of the limonene oxidation products with liquid chromatography coupled to the tandem mass spectrometry, Atmospheric Environment, 154, 297-307, https://doi.org/10.1016/j.atmosenv.2017.02.005, 2017.

Wotton, B. M., Gould, J. S., McCaw, W. L., Cheney, N. P., and Taylor, S. W.: Flame temperature and residence time of fires in dry eucalypt forest, International Journal of Wildland Fire, 21, 270-281, https://doi.org/10.1071/WF10127, 2012.

Xie, Q., Su, S., Chen, S., Xu, Y., Cao, D., Chen, J., Ren, L., Yue, S., Zhao, W., Sun, Y., Wang, Z., Tong, H., Su, H., Cheng, Y., Kawamura, K., Jiang, G., Liu, C. Q., and Fu, P.: Molecular characterization of firework-related urban aerosols using Fourier transform ion cyclotron resonance mass spectrometry, Atmos. Chem. Phys., 20, 6803-6820, https://doi.org/10.5194/acp-20-6803-2020, 2020.

Zhang, H., Yee, L. D., Lee, B. H., Curtis, M. P., Worton, D. R., Isaacman-VanWertz, G., Offenberg, J. H., Lewandowski, M., Kleindienst, T. E., Beaver, M. R., Holder, A. L., Lonneman, W. A., Docherty, K. S., Jaoui, M., Pye, H. O. T., Hu, W., Day, D. A., Campuzano-Jost, P., Jimenez, J. L., Guo, H., Weber, R. J., de Gouw, J., Koss, A. R., Edgerton, E. S., Brune, W., Mohr, C., Lopez-Hilfiker, F. D., Lutz, A., Kreisberg, N. M., Spielman, S. R., Hering, S. V., Wilson, K. R., Thornton, J. A., and Goldstein, A. H.: Monoterpenes are the largest source of summertime organic aerosol in the southeastern United States, Proceedings of the National Academy of Sciences, 115, 2038-2043, https://doi.org/10.1073/pnas.1717513115, 2018.

Zhao, Y., Thornton, J. A., and Pye, H. O. T.: Quantitative constraints on autoxidation and dimer formation from direct probing of monoterpene-derived peroxy radical chemistry, Proc Natl Acad Sci U S A, 115, 12142-12147, https://doi.org/10.1073/pnas.1812147115, 2018.